Preparing amorphous hydrophobic drug nanoparticles by nanoporous membrane extrusion

Aim: The aim of the present study was to develop a simple and straightforward method for formulating hydrophobic drugs into nanoparticulate form in a scalable and inexpensive manner. **Materials & methods:** The nanoporous membrane extrusion (NME) method was used to prepare hydrophobic drug nanoparticles. NME is based on the induced precipitation of drug-loaded nanoparticles at the exits of nanopores. Three common hydrophobic drug models (silymarin, β-carotene and butylated hydroxytoluene) were tested. The authors carefully investigated the morphology, crystallinity and dissolution profile of the resulting nanoparticles. **Results:** Using NME, the authors successfully prepared rather uniform drug nanoparticles (~100 nm in diameter). These nanoparticles were amorphous and show an improved dissolution profile compared with untreated drug powders. **Conclusion:** These studies suggest that NME could be used as a general method to produce nanoparticles of hydrophobic drugs.

Original submitted 8 June 2011; Revised submitted 7 May 2012

KEYWORDS: β-carotene ■ butylated hydroxytoluene ■ hydrophobic drug ■ nanoparticle ■ nanoporous membrane extrusion ■ silymarin ■ U-tube

Peng Guo[1,2,3], Tammy M Hsu[1], Yaping Zhao[1,4], Charles R Martin[2] & Richard N Zare*[1]

[1]Department of Chemistry, Stanford University, Stanford, CA 94305-5080, USA
[2]Department of Chemistry, University of Florida, Gainesville, FL 32611-7200, USA
[3]School of Engineering & Applied Sciences, Harvard University, Cambridge, MA 02138, USA
[4]School of Chemistry & Chemical Engineering, Shanghai Jiao Tong University, Shanghai, 200240, China
**Author for correspondence: Tel.: +1 650 723 3062 zare@stanford.edu*

More than 40% of drug-like compounds identified through combinatorial screening programs are poorly water soluble [1]. Their bioavailabilty in the human body is limited by their low saturation solubility and dissolution velocity. Common administration routes for hydrophobic drugs are limited to oral delivery, local injection, inhalation and surface retention, but not intravenous injection [2]. Intravenous injection is appealing because it has the highest bioavailabilty (almost 100%) among all administration routes with superior advantages in immediate effect, targeting effect and overcoming the first pass effect [3]. For example, the tumor targeting effect induced by intravenous administration has become a long-term interest of oncology [4]. Theoretically, hydrophobic drugs could be administrated by intravenous injection if they were formulated into particles sufficiently small enough to circulate in human vascular systems without causing immune reactions and embolism. Thus, nanotechnology may open the possibility for intravenous administration of hydrophobic drugs. Recently, a few groups have tried to intravenously deliver hydrophobic drugs using nanoparticle suspensions [5–7]. One famous example is that paclitaxel, an antitumor hydrophobic drug, which is bound to protein nanoparticles within an injectable suspension, was approved by the US FDA in 2005 and European Medicines Agency in 2008 for the treatment of breast cancer, which is the first clinical nanoparticle drug in the world [8]. Intravenous administration has very strict requirements on particle size of the nanoparticle suspension. Hydrophobic drug nanoparticles used for intravenous injection need to be well dispersed, small (~100 nm) and have a narrow size distribution. Although several fabrication methods have been developed to generate drug nanoparticles, such as nanoprecipitation [9], nanoemulsion [10] and ionic gelation [11], nevertheless, the need still exists to produce high-quality hydrophobic drug nanoparticles in a scalable, inexpensive manner.

Previous work in two laboratories, one at Stanford University (CA, USA), the other at the University of Florida (FL, USA), has featured the generation of such nanoparticles [12–21]. In this context, the authors developed a simple and efficient nanoporous membrane extrusion (NME) method that can prepare rather uniform 100 nm hydrophobic drug nanoparticles in a simple, low-cost manner. Three common hydrophobic drugs, silymarin (SM), β-carotene (BC) and butylated hydroxytoluene (BHT), were selected for the demonstration of nanoparticle formation. It has been shown that dissolution velocity of the resulting hydrophobic drug nanoparticles increases when they are made into a nanoparticulate form, caused by the increased

Future Medicine part of fsg

contact area between drug and solvent [22,23]. Meanwhile, other studies suggest that the subcelluar size of nanoparticles leads to a better cellular uptake both *in vivo* and *in vitro* [24,25]. Furthermore, converting the sample into an amorphous form could also increase hydrophobic bioavailability [26].

Materials & methods

SM and BC were purchased from MP Biomedicals (OH, USA) and BHT was purchased from Acros Organics (Geel, Belgium). The anodized aluminium oxide (AAO) membrane (20 and 200 nm on the entrance and exit sides) was obtained from Whatman Inc. (NJ, USA). All other chemicals were purchased from Sigma-Aldrich (MO, USA) in reagent grade and used as received.

Hydrophobic drug nanoparticle preparation

The experimental setup of the NME consists of two half U-tubes and an AAO nanoporous membrane, which is sandwiched between the two halves (Figure 1). The feed solution contained 25 mg of hydrophobic compound in 10 ml of organic solvent (SM and BHT were dissolved in acetone, and BC was dissolved in an acetone/tetrahydrofuran solution [50/50 v/v]). The receiver solution was 10 ml phosphate-buffered saline (PBS; pH 7.4) solution with 0.5 wt% Pluronic F68 detergent. One half of the U-tube was filled with 10 ml of feed solution and the other half was filled with 10 ml receiver solution. The feed soultion was driven through the nanoporous membrane by applying pressure (~2 psi) to it by connecting a compressed air outlet

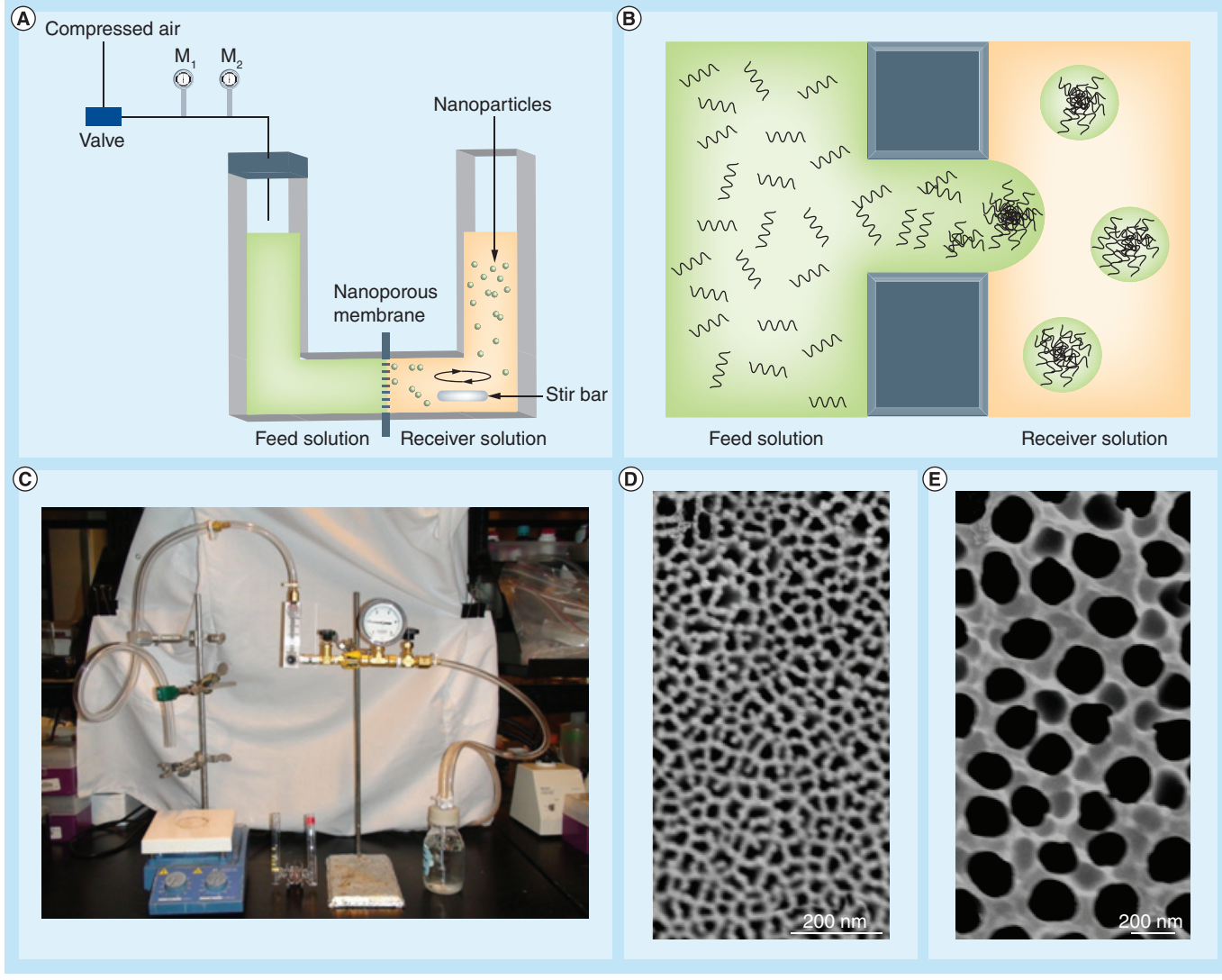

Figure 1. The nanoporous membrane extrusion method experimental setup. (A) The experimental setup where M_1 is the pressure meter and M_2 is the flow meter. **(B)** The particle-formation process. **(C)** Image of the experimental setup. Representive scanning electron microscope photograph of the anodized aluminium oxide membrane with **(D)** a 20 nm inlet and **(E)** a 200 nm outlet.

with a pressure meter to the feed solution of the U-tube. Vigorous magnetic stirring was used in the receiver solution to disperse the nanoparticles in the aqueous solution. The nanoparticles were collected from the receiver solution by filtration, rinsed three-times with deionized water and dried in the air at room temperature.

Scanning electron microscope

Morphologies of the obtained hydrophobic drug nanoparticles were characterized by a FEI XL30 Sirion scanning electron microscope (FEI Co., OR, USA). Dry samples on carbon sticky tape were sputter-coated for 90 s at 15 mA with Pd/Au.

Dynamic light-scattering measurement

Zetasizer Nano ZS (Malvern Instruments, PA, USA) was used to measure the hydrodynamic size, polydispersity index, and zeta potential of the hydrophobic drug nanoparticles. In the dynamic light-scattering (DLS) measurement, the nanoparticles were dispersed in the PBS (pH 7.4) with 0.5 wt% Pluronic F68 at a concentration of 0.1 mg/ml.

X-ray diffaction analysis

Powder x-ray diffraction (XRD) data of three hydrophobic drug nanoparticles and powders were recorded on a Scintag XDS2000 X-Ray Diffractometer (Scintage Inc., CA, USA) using filtered Cu Kα radiation (λ = 1.5406 Å) at 45 kV and 20 mA. XRD data were collected with a step scan with a step size of 0.040° and a step time of 1.0 s.

SM, BC and BHT nanoparticles used in XRD analysis were specifically prepared without using surfactant pluronic F68 in the receiver solution. This procedure makes sure that Pluronic F68 would not affect nanoparticle crystallinity in the XRD analysis.

Hydrophobic drug nanoparticle dissolution study

Dissolution profiles of SM and BHT nanoparticles and powders were carried out in PBS at pH 5.5 and 7.4. 1 ml SM or BHT nanoparticle or powder suspension (0.1 mg/ml in PBS with 0.5% Pluronic F68) was added to a dialysis tube (molecular weight cut-off: 1000). The dialysis tube was placed in a beaker with 30 ml PBS (pH 5.5 or 7.4). The beaker was then sealed with parafilm and incubated at 37°C on a shaker (100 rpm). For each time point, three 100 µl samples were collected from the solution outside of the dialysis tube and the absorbance intensity was measured on a SpectraMaxPlus 384 UV-Visible Spectrophotometer (Molecular Devices Corp, CA, USA). The SM and BHT absorbance wavelengths were 325 and 260 nm, respectively. The percentage of SM or BHT nanoparticles dissolved was defined as the sample aqueous concentration versus its saturated concentration.

Results

Figure 2 shows typical scanning electron microscopy images of SM, BC and BHT before and after the NME process. Figures 2A, 2D & 2G show SM, BC and BHT raw powders before NME processing. These powders have irregular shapes with a huge size distribution, ranging from a few hundred nanometers to a few hundred micrometers. Figures 2B, 2E & 2H show SM, BC and BHT nanoparticles post-NME. It is clear that hydrophobic drug powders were successfully formulated into nanoparticles by the NME process. The morphologies of these nanoparticles exhibit relatively spherical shapes at a mean diameter of 75 ± 27 nm (SM), 102 ± 23 nm (BC), and 130 ± 30 nm (BHT). The authors observed that the size of these hydrohpobic drug nanoparticles (75–130 nm) were smaller than the outlet diameter of the AAO nanopores (200 nm). This difference could be attributed to the rapid precipitation of feed solution droplets and the strong wall shear force by magnetic stirring, which caused nanoparticles to detach rapidly from the nanopore exits after solidification, preventing their continued growth. Size differences among the SM, BC and BHT nanoparticles were probably caused by the combination of the molecular weight and the structural complexity of each drug (Figure 3). It is well known that molecules with higher molecular weight and more complex chemical structures are usually easier to precipitate from a solvent. Different solidification velocities may have an effect on the final nanoparticle sizes. Using the experimental setup shown in Figure 1, the authors obtained 40 mg of SM nanoparticles within approximately 20 min.

Hydrophobic drug nanoparticles were also characterized by DLS measurements, from which it was found that the average hydrodynamic diameters of the SM, BC and BHT nanoparticles were 83, 105 and 132 nm, with a polydispersity index of 0.18, 0.238 and 0.234, respectively (Figures 2C, 2F & 2I). DLS results match closely with the particle size determined from scanning electron microscopy images. No nanoparticle agglomeration was detected in DLS, which

doi:10.2217/NNM.12.119

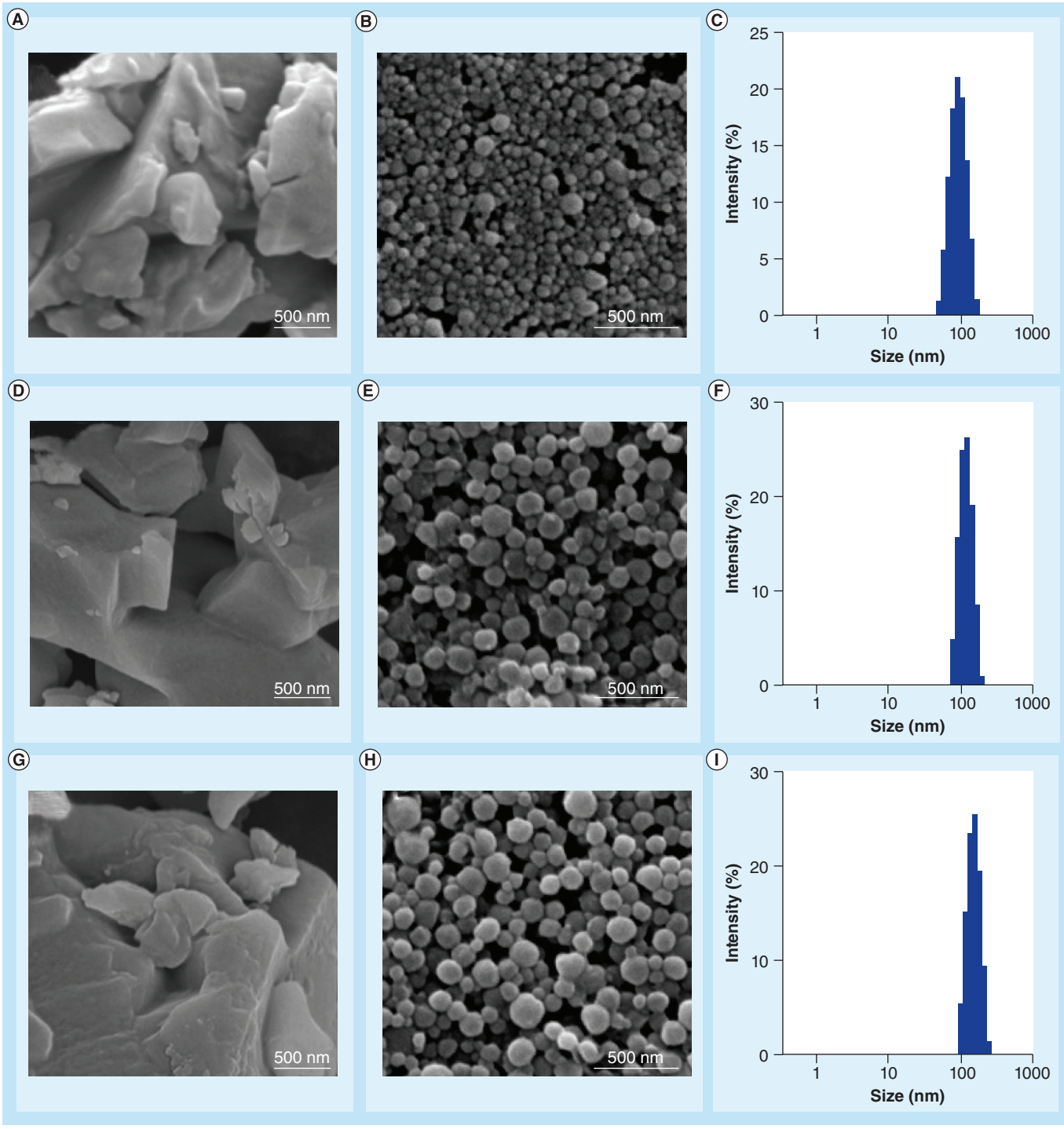

Figure 2. Scanning electron microscopy images before and after processing and dynamic light-scattering of nanoparticles. **(A–C)** Silymarin, **(D–F)** β-carotene and **(G–I)** butylated hydroxytoluene.

means that drug nanoparticles disperse readily in an aqueous environment. With the nonionic surfactant Pluronic F68 for stabilization, the drug nanoparticles express a slightly negative charge in PBS (pH 7.4) with zeta potentials of -3.3, -7.0 and -7.8 mV, respectively. During the NME process, we also observed that the flow rate over a certain range has little affect on the hydrodynamic radius of the nanoparticles. It was found that the smallest particle size (83 nm) was obtained at a flow rate of 1.5 ml $min^{-1}cm^{-2}$.

The appearance of the SM, BC and BHT nanoparticle suspensions was compared with the corresponding powder suspensions, as shown in Figure 4. The SM, BC and BHT nanoparticles were readily suspended in PBS (pH 7.4; 0.5 wt%

Pluronic F68) forming well-dispersed, stable and homogeneous suspensions. Hydrodynamic diameters of these nanoparticle suspensions were 79 (SM), 93 (BC) and 133 nm (BHT), respectively. These diameters were slightly different from those in Figure 2 because of batch-to-batch differences. The SM, BC and BHT powder suspensions were unstable and hetergeneous. Moreover, the powder agglomerates can be easily observed visually. From Figure 4, it seems that the powder suspensions look more transparent than nanoparticle suspensions, which is because most hydrophobic drug powders have already precipitated from solution and can be found at the bottom of the container. The authors also investigated the long-term stability of SM, BC and BHT nanoparticle suspensions in PBS at room temperature, and there was no obvious hydrodynamic size change during a 30-day period.

Powder XRD was used to determine the effect of the NME method on the crystallinity of the hydrophobic drug nanoparticles. Crystalline structures of pre-NME SM, BC and BHT powders and their post-NME nanoparticles are shown in Figure 5. Notable crystallinity changes in SM and BC were observed before and after NME processing. The pre-NME SM powders were a semi-crystalline material, exhibiting some peaks of medium intensity together with a strong background scattering phenomenon, in accordance with the results reported by others [27,28]. After the NME process, SM nanoparticles show a typical halo XRD pattern of amorphous materials. The reason is that the semi-crystalline SM powder was transformed into an amorphous phase during the NME process. A similar crystallinity change is also found in BC samples. Pre-NME BC powders exhibit strong diffraction peaks, whose 2θ values closely match the data in the powder diffraction database (JCPDS cards, No. 14-0912), indicating that the BC powder is a highly crystalline material. BC nanoparticles showed broad and diffuse diffraction patterns, the same as for the SM nanoparticles. Again, the authors conclude that the BC nanoparticles were in an amorphous state. In the BHT sample, both BHT powders and nanoparticles exist as amorphous solids; no sharp peaks of BHT were detected in the diffraction pattern. Thus, no obvious crystalline change was observed in BHT samples. All three hydrophobic nanoparticles prepared by the NME method were found to be in an amorphous state, which is important because amorphous materials demostrate significantly improved bioavalibalbity [26]. This behavior is believed to be the result of the higher internal energy of the metastable amorphous phase.

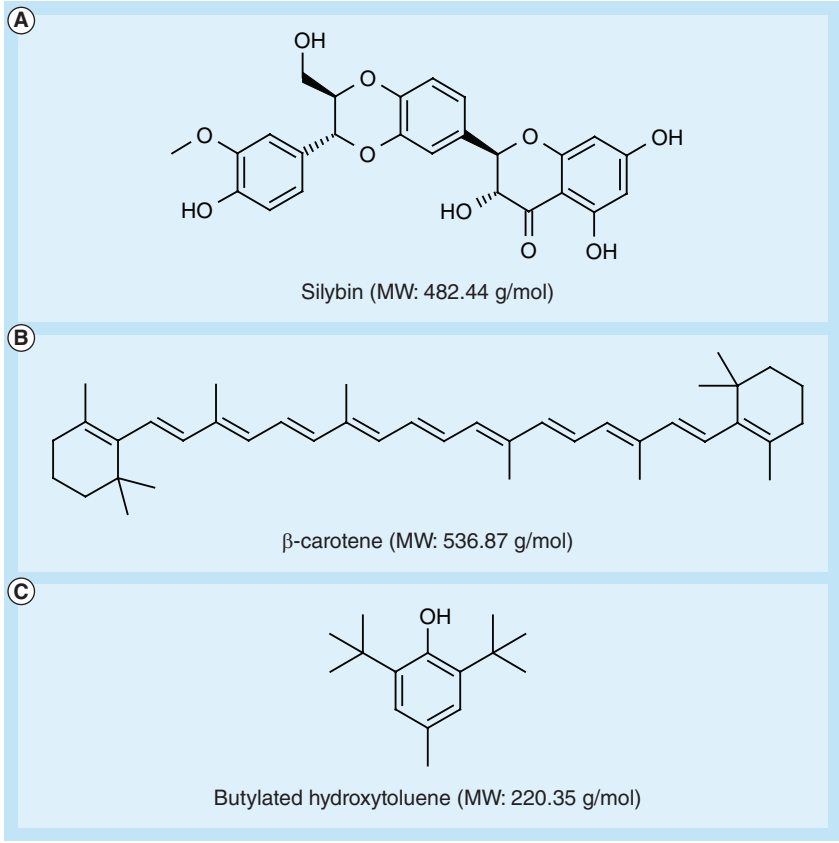

Figure 3. Chemical structures of hydrophobic compounds. (A) Silybin, **(B)** β-carotene and **(C)** butylated hydroxytoluene. Silybin is the major component in silymarin.
MW: Molecular weight.

Dissolution velocity is a crucial factor in hydrophobic drug delivery, which affects the hydrophobic drug biodistribution [29]. The authors determined and compared dissolution profiles for SM and BHT nanoparticles and powders in PBS at pH 7.4 and 5.5 in order to mimic the extra- and intra-cellular environments,

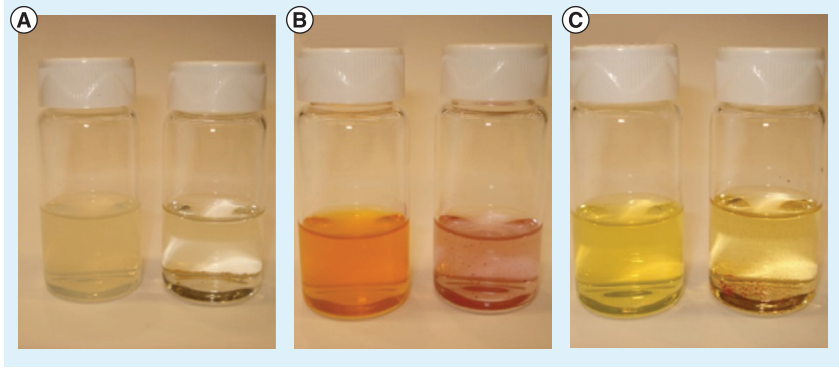

Figure 4. Comparisons of the appearance of the nanoparticle suspension (on the left) with the powder suspension (on the right). (A) Silymarin, **(B)** β-carotene and **(C)** butylated hydroxytoluene.

doi:10.2217/NNM.12.119

respectively. During *in vitro* or *in vivo* drug delivery, cells endocytose hydrophobic drug nanoparticles by transferring them into endosomes; the environment within endosomes is acidic [30]. All the dissolution profiles were characterized using UV adsorption. All test conditions were the same for both samples. FIGURES 6A & 6B show the dissolution profiles of SM nanoparticles and powder, respectively. The authors find that the dissolution velocity of SM nanoparticles is significantly faster than that of SM powder in both conditions. At 8 h, more than 90% of SM nanoparticles were dissolved compared with approximately 25% of untreated SM powder. The enhancement of the dissolution profile could be attributed to the increased surface area and amorphous nature of SM nanoparticles after NME processing. In BHT samples, the dissolution velocity of BHT nanoparticles was also faster than that of BHT powders. However, the difference between two dissolution velocites was much less marked than that observed for SM. The dissolution velocities of BHT nanoparticles and powder are almost the same in PBS at pH 5.5. The authors reason that BHT powder is also an amorphous material as described in FIGURE 5, and the amorphous nature of BHT powder greatly enhanced its dissolution velocity relative to the semi-crystalline SM powder.

Discussion

The authors' NME method is based on using a nanoporous membrane to separate two different solutions: a feed solution containing the dissolved hydrophobic compound; and a receiver solution in which the compound is insoluble (FIGURE 1). By pumping the feed solution through the nanoporous membrane into the receiver solution at a constant flow rate, hydrophobic drug nanodroplets are formed at the exits of the nanopores in contact with the receiver solution. The insolubility of the hydrophobic drug in the receiver solution causes nanodroplets at the nanopore exits to solidify into nanoparticles. The resulting nanoparticles were carried away from the nanopore exits by the continuous flow and become dispersed in the receiver solution. No clogging problems were encountered at the modest flow pressures used. The hydrophobic drug nanoparticles were then collected by filtration or centrifugation of the receiver solution.

The nanoporous membrane plays a key role in minimizing the size distribution of the nanoparticles and in preventing nanoparticle aggregation. For this purpose, membranes with uniform and well-defined nanopores are desired. Commercially available AAO (Whatman Inc.) was selected as the nanoporous membrane in the authors' experiment and appears to serve this

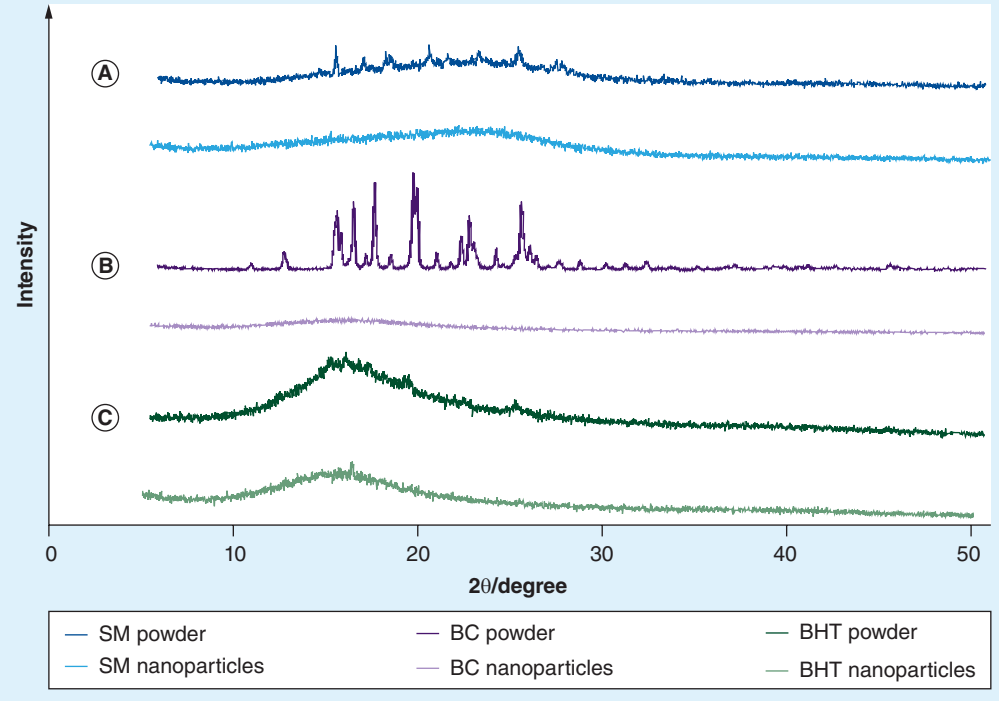

Figure 5. Powder x-ray diffraction patterns of nanoparticles in comparison with powders before nanoporous membrane extrusion. (A) SM, **(B)** BC and **(C)** BHT.
BC: β-carotene; BHT: Butylated hydroxytoluene; SM: Silymarin.

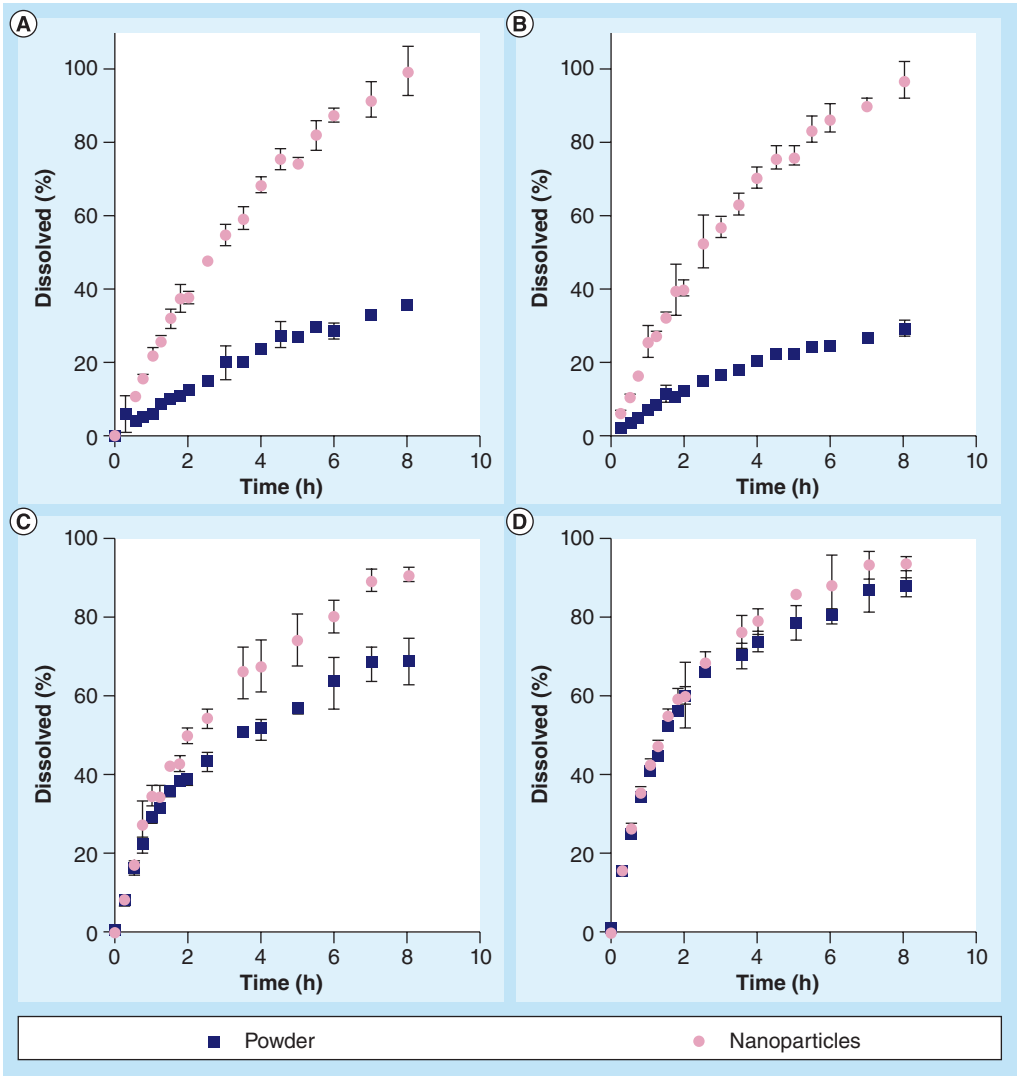

Figure 6. Dissolution profiles of silymarin and butylated hydroxytoluene nanoparticles and untreated powder in phosphate-buffered saline at 37°C. (A) Silymarin nanoparticles in phosphate-buffered saline at pH 7.4; **(B)** silymarin nanoparticles in phosphate-buffered saline at pH 5.5; **(C)** butylated hydroxytoluene nanoparticles in phosphate-buffered saline at pH 7.4; and **(D)** butylated hydroxytoluene nanoparticles in phosphate-buffered saline at pH 5.5. Percentage dissolved is defined as the sample aqueous concentration versus its saturated concentration. Error bars in each panel represent the standard deviation.

purpose well. The AAO membrane is 60 µm thick and contains 200 nm cylindrical pores at the face of the membrane in contact with the receiver solution and 20 nm pores in contact with the feed solution, as shown in Figure 1D. These 20 nm pores run parallel to one another for approximately 2 µm and then feed much larger pores (200 nm in diameter) that run parallel to one another through the remaining thickness of the membrane. The pore density of the AAO membrane at the exit (i.e., in contact with the receiver solution) is approximately $1.4 \times 10^9/cm^2$. In NME, the calculated flow velocity of feed solution through the AAO membrane is 55 µm/s. Considering that the thickness of the 20 nm AAO membrane is only 60 µm, the authors believe that the drug nanoparticles were most likely formed at the exits of 200 nm pores under rapid flow conditions.

Three hydrophobic drugs, SM, BC and BHT, were tested in this study. SM is a mixture of flavonolignans exacted from milk thistle, in which silybin is its major chemical constituent with hepatoprotective and anticancer clinical effects [31]. BC, a terpenoid compound, serves as a precursor to vitamin A in human and animal metabolism [32,33]. BHT is an antioxidant widely used as a food addictive [34]. All three drugs were sparingly solube in water: 0.25 mg/ml for SM, 0.6 mg/ml for BC and 1.1 µg/ml for BHT.

doi:10.2217/NNM.12.119

According to the literature, these molecules are nontoxic and are considered to be safe to use in the chemistry laboratory [31–34].

Particle size is enssential in hydrophobic drug delivery and biodistribulation. Previous studies in other particle systems have shown that the nanosuspension saturation solubilty, dissolution velocity, physical stability and biodistribution of nanoparticles are strongly dependent on the nanoparticle hydrodynamic diameter [24,25,35,36]. In the human body, the smallest human blood vessels, blood capillaries, are approximately 5 µm in diameter. If the particle size is larger than 5 µm, it may lead to severe blood capillary blockade and embolism [37]. Therefore, all injectable nanoparticle suspensions strictly control the particle size to be smaller than 5 µm. Furthermore, the phagocytic cells of the immune system (e.g., macrophages) recognize and uptake nanoparticles larger than 200 nm [38], causing an immune response and sabotaging drug bioavailabilty and efficacy. As a result, nanoparticles with a hydrodynamic size less than 200 nm are generally considered to be optimal for intravenous injection [39,40]. The authors' hydrophobic drug nanoparticles (83–132 nm) prepared by the NME method fall in this acceptable range. In tumor therapy, nanoparticles with a size less than 200 nm can passively accumulate within tumors by the enhanced permeability and retention effect. This tumor targeting effect is ubiquitously adapted in antitumor therapy [4]. Thus, the authors believe that their NME process is a general and effective means of producing nanoparticles of hydrophobic drugs.

Conclusion

The authors have developed a NME method that can prepare hydrophobic drug nanoparticles in a simple and low-cost manner. The resulting hydrophobic drug nanoparticles are converted into an amorphous phase. Dissolution profiles show that hydrophobic drug nanoparticles dissolve much faster than untreated drug powders owing to the increased surface area and amorphous nature of the resulting nanoparticles. The uniform size and shape control of drug nanoparticles at a high production rate suggest that the NME method is applicable to a wide class of poorly water-soluble drugs and the resulting nanoparticles enhance drug solubility.

Financial & competing interests disclosure

The authors thank the National Science Foundation (CBET-0827806) for supporting this project. The authors have no other relevant affiliations or financial involvement with any organization or entity with a financial interest in or financial conflict with the subject matter or materials discussed in the manuscript. This includes employment, consultancies, honoraria, stock ownership or options, expert testimony, grants or patents received or pending, or royalties.

No writing assistance was utilized in the production of this manuscript.

Ethical conduct of research

The authors state that they have obtained appropriate institutional review board approval or have followed the principles outlined in the Declaration of Helsinki for all human or animal experimental investigations. In addition, for investigations involving human subjects, informed consent has been obtained from the participants involved.

Executive summary

- The authors successfully developed a simple and low-cost method to formulate hydrophobic drugs into nanoparticulate form with small size (~100 nm) and rather uniform distribution in size.
- Hydrophobic drug nanoparticles prepared by nanoporous membrane extrusion were converted into an amorphous phase.
- Dissolution profiles of hydrophobic drugs were improved by formulating them into nanoparticulate form.

References

Papers of special note have been highlighted as:
- of interest
- of considerable interest

1 Lipinski CA. Drug-like properties and the causes of poor solubility and poor permeability. *J. Pharmacol. Toxicol. Methods* 44(1), 235–249 (2000).

- **Discusses the problems caused by poor drug solubility.**

2 Cooper ER. Nanoparticles: a personal experience for formulating poorly water soluble drugs. *J. Control. Release* 141(3), 300–302 (2010).

- **Discusses the problems caused by poor drug solubility and the difficulties in overcoming this obstacle.**

3 Gao L, Zhang D, Chen M. Drug nanocrystals for the formulation of poorly soluble drugs and its application as a potential drug delivery system. *J. Nanopart. Res.* 10(5), 845–862 (2008).

4 Maeda H. The enhanced permeability and retention (EPR) effect in tumor vasculature: the key role of tumor-selective macromolecular drug targeting. *Adv. Enzyme Regul.* 41, 189–207 (2001).

5 Gradishar WJ. Phase III trial of nanoparticle albumin-bound paclitaxel compared with polyethylated castor oil-based paclitaxel in women with breast cancer. *J. Clin. Oncol.* 23(31), 7794–7803 (2005).

- **Use of nanoparticles for delivering hydrophobic drugs.**

6 Baba K, Pudavar HE, Roy I *et al.* New method for delivering a hydrophobic drug for photodynamic therapy using pure nanocrystal form of the drug. *Mol. Pharm.* 4(2), 289–297 (2007).

▪ **Use of nanoparticles for delivering hydrophobic drugs.**

7 Peters K, Leitzke S, Diederichs JE *et al.* Preparation of a clofazimine nanosuspension for intravenous use and evaluation of its therapeutic efficacy in murine *Mycobacterium avium* infection. *J. Antimicrob. Chemother.* 45(1), 77–83 (2000).

▪ **Use of nanoparticles for delivering hydrophobic drugs.**

8 Wagner V, Dullaart A, Bock A-K, Zweck A. The emerging nanomedicine landscape. *Nat. Biotechnol.* 24(10), 1211–1217 (2006).

9 Legrand P, Lesieur S, Bochot A *et al.* Influence of polymer behaviour in organic solution on the production of polylactide nanoparticles by nanoprecipitation. *Int. J. Pharm.* 344(1–2), 33–43 (2007).

10 Antonietti M. Polyreactions in miniemulsions. *Prog. Polym. Sci.* 27(4), 689–757 (2002).

11 Tokumitsu H, Ichikawa H, Fukumori Y. Chitosan-gadopentetic acid complex nanoparticles for gadolinium neutron-capture therapy of cancer: preparation by novel emulsion-droplet coalescence technique and characterization. *Pharm. Res.* 16(12), 1830–1835 (1999).

12 Jacobson GB, Shinde R, Contag CH, Zare RN. Sustained release of drugs dispersed in polymer nanoparticles. *Angew. Chem. Int. Ed.* 47(41), 7880–7882 (2008).

13 Jacobson GB, Gonzalez-Gonzalez E, Spitler R *et al.* Biodegradable nanoparticles with sustained release of functional siRNA in skin. *J. Pharm. Sci.* 99(10), 4261–4266 (2010).

14 Jacobson GB, Shinde R, McCullough RL *et al.* Nanoparticle formation of organic compounds with retained biological activity. *J. Pharm. Sci.* 99(6), 2750–2755 (2010).

15 Guo P, Martin CR, Zhao Y, Ge J, Zare RN. General method for producing organic nanoparticles using nanoporous membranes. *Nano Lett.* 10(6), 2202–2206 (2010).

▪▪ **The first example of nanoporous membrane extrusion for nanoparticle formation.**

16 Ge J, Jacobson GB, Lobovkina T, Holmberg K, Zare RN. Sustained release of nucleic acids from polymeric nanoparticles using microemulsion precipitation in supercritical carbon dioxide. *Chem. Commun. (Camb.)* 46(47), 9034–9036 (2010).

17 Buyukserin F, Medley CD, Mota MO *et al.* Antibody-functionalized nano test tubes target breast cancer cells. *Nanomedicine (Lond.)* 3(3), 283–292 (2008).

18 Buyukserin F, Kang M, Martin CR. Plasma-etched nanopore polymer films and their use as templates to prepare "nano test tubes." *Small* 3(1), 106–110 (2007).

19 Hillebrenner H, Buyukserin F, Stewart JD, Martin CR. Template synthesized nanotubes for biomedical delivery applications. *Nanomedicine* 1(1), 39–50 (2006).

20 Hillebrenner H, Buyukserin F, Kang M, Mota MO, Stewart JD, Martin CR. Corking nano test tubes by chemical self-assembly. *J. Am. Chem. Soc.* 128(13), 4236–4237 (2006).

21 Maas M, Guo P, Keeney M *et al.* Preparation of mineralized nanofibers: collagen fibrils containing calcium phosphate. *Nano Lett.* 11(3), 1383–1388 (2011).

▪▪ **The first example of nanoporous membrane extrusion for nanofiber formation and its biomedical applications.**

22 Liversidge G. Particle size reduction for improvement of oral bioavailability of hydrophobic drugs: I. Absolute oral bioavailability of nanocrystalline danazol in beagle dogs. *Int. J. Pharm.* 125(1), 91–97 (1995).

▪ **Study of nanoparticle size on bioavailability for hydrophobic drug delivery.**

23 Müller R. Nanosuspensions for the formulation of poorly soluble drugs I. Preparation by a size-reduction technique. *Int. J. Pharm.* 160(2), 229–237 (1998).

24 Panyam J. Biodegradable nanoparticles for drug and gene delivery to cells and tissue. *Adv. Drug Deliv. Rev.* 55(3), 329–347 (2003).

25 Farokhzad OC. Targeted nanoparticle-aptamer bioconjugates for cancer chemotherapy *in vivo*. *Proc. Natl Acad. Sci. USA* 103(16), 6315–6320 (2006).

26 Hancock BC, Zografi G. Characteristics and significance of the amorphous state in pharmaceutical systems. *J. Pharm. Sci.* 86(1), 1–12 (1997).

27 Sun N, Zhang X, Lu Y, Wu W. *In vitro* evaluation and pharmacokinetics in dogs of solid dispersion pellets containing *Silybum marianum* extract prepared by fluid-bed coating. *Planta Med.* 74(2), 126–132 (2008).

28 Wang Y, Zhang D, Liu Z *et al. In vitro* and *in vivo* evaluation of silybin nanosuspensions for oral and intravenous delivery. *Nanotechnology* 21(15), 155104 (2010).

29 Rabinow BE. Nanosuspensions in drug delivery. *Nat. Rev. Drug Discov.* 3(9), 785–796 (2004).

30 You J-O, Almeda D, Ye GJ, Auguste DT. Bioresponsive matrices in drug delivery. *J. Biol. Eng.* 4(1), 15 (2010).

31 Ferenci P, Dragosics B, Dittrich H *et al.* Randomized controlled trial of silymarin treatment in patients with cirrhosis of the liver. *J. Hepatol.* 9(1), 105–113 (1989).

32 Omenn GS, Goodman GE, Thornquist MD *et al.* Effects of a combination of beta carotene and vitamin A on lung cancer and cardiovascular disease. *N. Engl. J. Med.* 334(18), 1150–1155 (1996).

33 Burton G, Ingold K. beta-Carotene: an unusual type of lipid antioxidant. *Science* 224(4649), 569–573 (1984).

34 Branen AL. Toxicology and biochemistry of butylated hydroxyanisole and butylated hydroxytoluene. *J. Am. Oil Chem. Soc.* 52(2), 59–63 (1975).

35 Yinwin K, Feng S. Effects of particle size and surface coating on cellular uptake of polymeric nanoparticles for oral delivery of anticancer drugs. *Biomaterials* 26(15), 2713–2722 (2005).

36 Chithrani BD, Ghazani AA, Chan WCW. Determining the size and shape dependence of gold nanoparticle uptake into mammalian cells. *Nano Lett.* 6(4), 662–668 (2006).

37 Müller RH, Jacobs C, Kayser O. Nanosuspensions as particulate drug formulations in therapy. Rationale for development and what we can expect for the future. *Adv. Drug Deliv. Rev.* 47(1), 3–19 (2001).

38 Moghimi SM, Hunter AC, Murray JC. Long-circulating and target-specific nanoparticles: theory to practice. *Pharmacol. Rev.* 53(2), 283–318 (2001).

39 Wong J, Brugger A, Khare A *et al.* Suspensions for intravenous (IV) injection: a review of development, preclinical and clinical aspects. *Adv. Drug Deliv. Rev.* 60(8), 939–954 (2008).

40 Gupta AK, Gupta M. Synthesis and surface engineering of iron oxide nanoparticles for biomedical applications. *Biomaterials* 26(18), 3995–4021 (2005).

doi:10.2217/NNM.12.119